ЖЭТФ, 2010, том 137, вып. 1, стр. 24–32 

# RADIATIVE RECOIL CORRECTIONS TO HYPERFINE SPLITTING: POLARIZATION INSERTIONS IN THE ELECTRON FACTOR

*M. I. Eides* [a*], *V. A. Shelyuto* [b**]

[a] *Department of Physics and Astronomy, University of Kentucky KY 40506, Lexington, USA*

[b] *Mendeleev Institute of Metrology 190005, St. Petersburg, Russia*

Received July 9, 2009

We consider three-loop radiative recoil corrections to hyperfine splitting in muonium due to insertions of the one-loop polarization operator in the electron factor. The contribution generated by electron polarization insertions is a cubic polynomial in the large logarithm of the electron–muon mass ratio. The leading logarithm cubed and logarithm squared terms are well known for some time. We calculate all single-logarithmic and nonlogarithmic radiative recoil corrections of the order $\alpha^3(m/M)E_F$ generated by diagrams with the electron and muon polarization insertions.

## 1. INTRODUCTION

Leading three-loop logarithm cubed and logarithm squared radiative recoil contributions to hyperfine splitting (HFS) in muonium were calculated long time ago (see, e.g., reviews [1, 2]). Recently, we started the calculation of all single-logarithmic and nonlogarithmic radiative recoil corrections (see review [3]). Below, we consider single-logarithmic and nonlogarithmic radiative recoil corrections due to insertions of electron and muon polarization operators in the radiative photon line, shown in Figs. 1 and 2.

Three-loop diagrams in Figs. 1 and 2 can be obtained from the diagrams with two-photon exchanges by insertion of radiative corrections in Fig. 3. The two-photon diagrams in Fig. 3 produce the leading radiative recoil correction when the loop momentum is much larger than the electron mass, and the insertion of a radiative correction can only increase the integration momentum. Therefore, calculating the diagrams in Figs. 1 and 2 we may forget about external virtualities and calculate matrix elements in the scattering regime between the free electron and muon spinors. To turn the matrix element into contribution to HFS, we

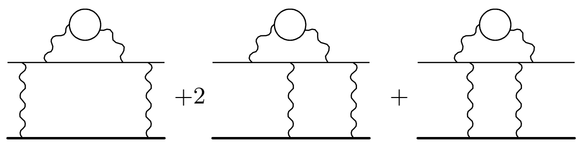

**Fig. 1.** Electron polarization insertions

multiply the scattering matrix element by the squared Coulomb–Schrödinger bound state wave function at the origin and calculate the difference between spin-one and spin-zero states. We use the Feynman gauge to obtain matrix elements of the gauge invariant sets of diagrams in Figs. 1 and 2. Each of the diagrams in Figs. 1 and 2 contains a polarization operator insertion in one of the radiative photon lines. We account for this insertion using the massive photon propagator for radiative photons (but not for exchanged photons) with the photon mass squared

$$\lambda^2 = \frac{4m^2}{1-v^2}$$

or

$$\lambda^2 = \frac{4M^2}{1-v^2},$$

where $m$ and $M$ respectively are the electron and muon masses. Insertion of the polarization operator in the

*Also at Petersburg Nuclear Physics Institute, 188300, Gatchina, St. Petersburg Russia; E-mail: eides@pa.uky.edu, eides@thd.pnpi.spb.ru

**E-mail: shelyuto@vniim.ru

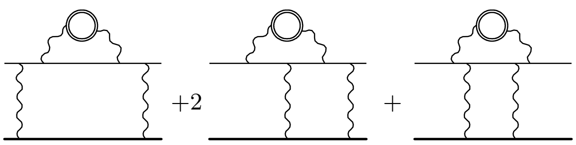

**Fig. 2.** Muon polarization insertions

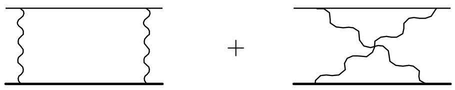

**Fig. 3.** Two-photon exchanges

radiative photon line is accompanied by an additional integration over velocity $v$ with the weight

$$\int_0^1 \frac{dv}{1-v^2}\, v^2 \left(1-\frac{v^2}{3}\right). \tag{1}$$

Besides single-logarithmic and nonlogarithmic contributions, the diagrams in Fig. 1 also generate well known much larger nonrecoil and logarithm-squared recoil contributions [1]. We calculate the contributions of the diagrams in Figs. 1 and 2 with linear accuracy in the small electron–muon mass ratio $m/M$. In particular, we reproduce the nonrecoil and logarithm-squared recoil contributions, which serves as an additional check of our new results. The paper is organized as follows. In Sect. 2, we describe calculations of the diagrams with the electron polarizations in Fig. 1, and Sect. 3 deals with the diagrams with the muon polarizations in Fig. 2. The results are collected in the last section.

## 2. ELECTRON POLARIZATION OPERATOR

### 2.1. Calculation of the mass operator contribution

We calculate matrix elements of each of the diagrams in Fig. 1 separately. The respective integrals can be obtained by inserting radiative corrections in the expression for the contribution of the skeleton diagrams in Fig. 3 to HFS. Contribution of the diagram with the self-energy insertion in Fig. 1 has the form (cf. [4])

$$\begin{aligned}\Delta\epsilon_\Sigma &= \frac{3i}{8\pi^2\mu^2}\int_0^1 dx\int_0^x dy\int_0^1 \frac{dv}{1-v^2}v^2\left(1-\frac{v^2}{3}\right)\times\\ &\times\int\frac{d^4k}{k^4}\frac{2k^2}{k^4-\mu^{-2}k_0^2}\,\frac{1}{-k^2+2k_0+a_1^2(x,y)-i0}\times\\ &\times\left[h_1(x,y)k_0-\frac{h_2(x,y)}{3}(2k^2+k_0^2)\right]\equiv\\ &\equiv\Delta\epsilon_{\Sigma1}+\Delta\epsilon_{\Sigma2},\end{aligned} \tag{2}$$

where the dimensionless energy $\Delta\epsilon_\Sigma$ is related to the energy shift $\Delta E_\Sigma$ as[1)]

$$\Delta E_\Sigma = \frac{\alpha^2(Z\alpha)}{\pi^3}\,\frac{m}{M}E_F\Delta\epsilon_\Sigma,$$

$\mu = m/(2M)$, $k$ is the dimensionless Minkowski exchange momentum, $\Delta\epsilon_{\Sigma1}$ and $\Delta\epsilon_{\Sigma2}$ are the integrals corresponding to the two terms in the square brackets, and

$$\begin{aligned} h_1(x,y) &= \frac{1+x}{y},\\ h_2(x,y) &= \frac{1-x}{y}\left[1-\frac{2(1+x)y}{x^2+\lambda^2(1-x)}\right],\\ a_1^2(x,y) &= \frac{x^2+\lambda^2(1-x)}{(1-x)y}.\end{aligned} \tag{3}$$

The integration over $v$ in Eq. (2) accounts for the electron loop that is included in the integrand via the finite mass $\lambda = \sqrt{4/(1-v^2)}$ of the radiative photon. We calculate two leading terms in the expansion of the dimensionless energy $\Delta\epsilon_\Sigma$ in Eq. (2) with respect to the small parameter $\mu$ (the term of the order $1/\mu$ and the term independent of $\mu$).

#### 2.1.1. Nonrelativistic contribution

As a first step of the calculation, we obtain the leading term of the order $1/\mu$ from the expression for $\Delta\epsilon_\Sigma$ in Eq. (2). This term gives the leading nonrecoil contribution to HFS and arises, as all nonrecoil contributions, in the external field approximation. To extract the nonrecoil contribution from the expression in Eq. (2), we take the residue at the muon pole, which with a linear accuracy in $\mu$ amounts to the substitution

$$\frac{2k^2}{k^4-\mu^{-2}k_0^2} \to -2\pi i\mu\delta(k_0-\mu\mathbf{k}^2). \tag{4}$$

Then we obtain the nonrelativistic contribution for the muon in the form

1) The Fermi energy is defined as $E_F = (8/3)(Z\alpha)^4(m/M)m$.

$$\Delta\epsilon_\Sigma(NR) = \frac{3}{4\pi\mu}\int_0^1 dx\int_0^x dy\int_0^1 \frac{dv}{1-v^2}v^2\left(1-\frac{v^2}{3}\right)\times \times\int\frac{d^3k}{\mathbf{k}^2[\mathbf{k}^2(1+2\mu)+a_1^2(x,y)]}\times \times\left[\mu h_1(x,y)+\frac{2}{3}h_2(x,y)\right]. \quad (5)$$

This last integral contains both recoil and nonrecoil contributions. The recoil contribution is be treated on equal grounds with other recoil contributions considered below. Integrating over the momentum in Eq. (5) and expanding the result with respect to the small parameter $\mu$, we obtain

$$\Delta\epsilon_\Sigma(NR) = \int_0^1 dx\int_0^x dy\int_0^1 \frac{dv}{1-v^2}v^2\left(1-\frac{v^2}{3}\right)\times \times\left[\frac{1}{\mu}\frac{\pi}{a_1(x,y)}h_2(x,y)+ + \frac{\pi}{2a_1(x,y)}(3h_1(x,y)-2h_2(x,y))\right] = = \frac{0.4462}{\mu}+2.2372\equiv\Delta\epsilon_\Sigma^{(\mu)}(NR)+\Delta\epsilon_\Sigma^{(c)}(NR). \quad (6)$$

### 2.1.2. $\mu$- and $c$-integrals

We return to the calculation of the first two terms in the expansion of the contributions to HFS in Eq. (2) with respect to $\mu$. An attempt to calculate the integral in Eq. (2) with the help of Feynman parameters leads to the integrands that do not admit expansion in the small parameter $\mu$ before the integration. Therefore, we use another approach to the calculation of the integral in Eq. (2) (as well as to the calculation of other integrals of this type below), and directly integrate over the exchange momentum $k$ in four-dimensional polar coordinates. After the Wick rotation and integration over angles (and omitting some higher-order terms in $\mu$), we obtain an integral representation for the contributions $\Delta\epsilon_{\Sigma 1}$ and $\Delta\epsilon_{\Sigma 2}$ defined in Eq. (2). The integral representation for $\Delta\epsilon_{\Sigma 1}$ (cf. [5]) is

$$\Delta\epsilon_{\Sigma 1} = -3\int_0^1 dx\int_0^x dy\int_0^1 \frac{dv}{1-v^2}v^2\left(1-\frac{v^2}{3}\right)h_1(x,y)\times \times\int_0^\infty dk^2\left\{\frac{1}{(k^2+a_1^2)^2}\left(\mu k\sqrt{1+\mu^2k^2}-\mu^2k^2\right)- -\frac{1}{4k^2}\left[\frac{1}{k^2+a_1^2}\sqrt{(k^2+a_1^2)^2+4k^2}-1\right]\right\}, \quad (7)$$

and the integral representation for $\Delta\epsilon_{\Sigma 2}$ (cf. [4]) is

$$\Delta\epsilon_{\Sigma 2} = \int_0^1 dx\int_0^x dy\int_0^1 \frac{dv}{1-v^2}v^2\left(1-\frac{v^2}{3}\right)h_2(x,y)\times \times\int_0^\infty dk^2\left\{\frac{1}{k^2+a_1^2}\left[\frac{1}{\mu k}\sqrt{1+\mu^2k^2}- -\frac{1}{2}\left(\mu k\sqrt{1+\mu^2k^2}-\mu^2k^2\right)\right]+ +\left[-\frac{\sqrt{(k^2+a_1^2)^2+4k^2}}{(k^2+a_1^2)^2}+ +\frac{1}{8k^2}\left(\sqrt{(k^2+a_1^2)^2+4k^2}-(k^2+a_1^2)\right)\right]\right\}. \quad (8)$$

Each integrand in Eq. (7) and Eq. (8) is a sum of $\mu$-dependent and $\mu$-independent integrals, and we calculate them separately. While both integrals are convergent, a naive separation of $\mu$-dependent and $\mu$-independent terms in the integrands sometimes leads to integrals that are ultravioletly divergent at large integration momenta $k$. For example, the integral over $k$ of the $\mu$-dependent term in the integrand in Eq. (7) converges at large integration momenta, while the respective integral in Eq. (8) diverges. This divergence arises because $\mu$-dependent terms in the integrand become $\mu$-independent constants at high momenta. In such cases, we redefine the $\mu$-dependent terms in the integrand by subtracting the leading asymptotic constant, and add this constant to the $\mu$-independent terms in the integrand. A universal recipe for such restructuring of the integrands in Eqs. (7) and (8) is described by the substitutions

$$\frac{1}{\mu k}\sqrt{1+\mu^2k^2}\to\frac{1}{\mu k}\left(\sqrt{1+\mu^2k^2}-\mu k\right), \left(\mu k\sqrt{1+\mu^2k^2}-\mu^2k^2\right)\to \to\left(\mu k\sqrt{1+\mu^2k^2}-\mu^2k^2-\frac{1}{2}\right). \quad (9)$$

We subtract 1 in the first case, and 1/2 in the second case. In both cases, we add the terms corresponding to these constants to the $\mu$-independent terms in the integrands. After this restructuring (when needed), we write integrals (7) and (8) as sums of what we call $\mu$- and $c$-integrals,

$$\Delta\epsilon = \Delta\epsilon^{(\mu)}+\Delta\epsilon^{(c)}. \quad (10)$$

We consider first the calculation of the $\mu$-integrals. The integral over $k$ in Eq. (7) converges, the integrand does not require any restructuring, and the $\mu$-integral has the form

$$\Delta\epsilon^{(\mu)}_{\Sigma 1} = -3\int\limits_0^1 dx\int\limits_0^x dy\int\limits_0^1 \frac{dv}{1-v^2}v^2\left(1-\frac{v^2}{3}\right)h_1(x,y)\times$$
$$\times\int\limits_0^\infty \frac{dk^2}{(k^2+a_1^2)^2}\left(\mu k\sqrt{1+\mu^2k^2}-\mu^2k^2\right). \quad (11)$$

This integral is of the order $\mu$, and therefore, with our accuracy, it does not give any contribution

$$\Delta\epsilon^{(\mu)}_{\Sigma 1} = 0. \quad (12)$$

We next calculate the $\mu$-integral arising from the integral in Eq. (8):

$$\Delta\epsilon^{(\mu)}_{\Sigma 2} = \int\limits_0^1 dx\int\limits_0^x dy\int\limits_0^1 \frac{dv}{1-v^2}v^2\left(1-\frac{v^2}{3}\right)h_2(x,y)\times$$
$$\times\int\limits_0^\infty dk^2\frac{1}{k^2+a_1^2}\left[\frac{1}{\mu k}\left(\sqrt{1+\mu^2k^2}-\mu k\right)-\right.$$
$$\left.-\frac{1}{2}\left(\mu k\sqrt{1+\mu^2k^2}-\mu^2k^2-\frac{1}{2}\right)\right]. \quad (13)$$

Unlike in the case of $\Delta\epsilon^{(\mu)}_{\Sigma 1}$, the naive integral over $k$ of the $\mu$-dependent terms in Eq. (8) diverges at large $k$, and we restructure the integrand in accordance with Eq. (9). Besides the recoil contribution, the integral in Eq. (13) also contains the nonrelativistic contribution $\Delta\epsilon^{(\mu)}_{\Sigma}(NR)$ that we calculated separately in Eq. (5). This nonrelativistic contribution is generated by the leading $1/(\mu k)$ term in the small-$\mu k$ expansion of the expression in the square brackets in Eq. (13). It coincides with the contribution generated by the first term in the square brackets in Eq. (6). To avoid double counting, we subtract this contribution from the integrand in Eq. (13) by the substitution

$$\frac{1}{\mu k}\sqrt{1+\mu^2k^2}\to\frac{1}{\mu k}\left(\sqrt{1+\mu^2k^2}-1\right) \quad (14)$$

in the integrand. This substitution gives a universal recipe for subtracting the nonrecoil corrections in all $\mu$-integrals to be considered below. We emphasize that it is needed only in the first of the two typical structures with square roots in Eq. (9) that arise in the expressions for $\mu$-integrals. The leading term in the small-$\mu k$ expansion of the second structure is nonsingular and does not generate a nonrecoil contribution.

Finally, the second $\mu$-integral for the mass operator insertion in the electron line has the form

$$\Delta\epsilon^{(\mu)}_{\Sigma 2} - \Delta\epsilon^{(\mu)}_{\Sigma 2}(NR) = \int\limits_0^1 dx\int\limits_0^x dy\ \times$$
$$\times\int\limits_0^1 \frac{dv}{1-v^2}v^2\left(1-\frac{v^2}{3}\right)h_2(x,y)\int\limits_0^\infty\frac{dk^2}{k^2+a_1^2}\times$$
$$\times\left[\frac{1}{\mu k}\left(\sqrt{1+\mu^2k^2}-\mu k-1\right)-\right.$$
$$\left.-\frac{1}{2}\left(\mu k\sqrt{1+\mu^2k^2}-\mu^2k^2-\frac{1}{2}\right)\right]. \quad (15)$$

Other integrals of this type arise in calculations of other contributions to HFS below. To extract the first term in the small-$\mu$ expansion of integrals of this type, we introduce an auxiliary parameter $\sigma$, such that $1\ll\sigma\ll 1/\mu$ (see, e.g., [6, 4]). Then we separate the large and small integration momenta regions with the help of this parameter $\sigma$ and use different approximations in the different regions. In the region of small integration momenta $0\le k\le\sigma$, we expand the integrand with respect to $\mu k\ll 1$ and obtain

$$\Delta\epsilon^{(\mu<)}_{\Sigma 2} - \Delta E^{(\mu<)}_{\Sigma 2}(NR) \approx -\frac{1}{6}\ln^3\sigma+\frac{19}{24}\ln^2\sigma+$$
$$+\left(-\pi^2+\frac{589}{72}\right)\ln\sigma + 1.3220. \quad (16)$$

In the region of large integration momenta $k\le\sigma$, we expand the integrand with respect to $1/k\ll 1$ and obtain

$$\Delta\epsilon^{(\mu>)}_{\Sigma 2} - \Delta\epsilon^{(\mu>)}_{\Sigma 2}(NR) \approx \frac{1}{6}\ln^3(2\mu)+\frac{1}{24}\ln^2(2\mu)+$$
$$+\left(\frac{13\pi^2}{12}-\frac{335}{36}\right)\ln(2\mu)+\frac{1}{4}\zeta(3)-\frac{215\pi^2}{144}+$$
$$+\frac{103}{8}+\frac{1}{6}\ln^3\sigma-\frac{19}{24}\ln^2\sigma+\left(\pi^2-\frac{589}{72}\right)\ln\sigma. \quad (17)$$

In the intermediate region $k\sim\sigma$, both approximations $\mu k\ll 1$ and $1/k\ll 1$ are valid simultaneously, and all dependence on the auxiliary parameter $\sigma$ cancels in the sum of the contributions in Eq. (16) and Eq. (17):

$$\Delta\epsilon^{(\mu)}_{\Sigma 2} - \Delta\epsilon^{(\mu)}_{\Sigma 2}(NR) \approx \frac{1}{6}\ln^3(2\mu)+\frac{1}{24}\ln^2(2\mu)+$$
$$+\left(\frac{13\pi^2}{12}-\frac{335}{36}\right)\ln(2\mu)+\frac{1}{4}\zeta(3)-\frac{215\pi^2}{144}+$$
$$+\frac{103}{8}+1.3220. \quad (18)$$

We next turn to the $c$-integrals defined in Eqs. (10), (7), and (8). We easily perform the momentum integration in the integral for $\Delta\epsilon^{(c)}_{\Sigma 1}$,

$$\Delta\epsilon^{(c)}_{\Sigma 1} = \frac{3}{4}\int_0^1 dx\int_0^x dy\int_0^1 \frac{dv}{1-v^2}v^2\left(1-\frac{v^2}{3}\right)h_1(x,y)\times \int_0^\infty \frac{dk^2}{k^2}\left[\frac{1}{k^2+a_1^2}\sqrt{(k^2+a_1^2)^2+4k^2}-1\right] = 3\int_0^1 dx\int_0^x dy\int_0^1 \frac{dv}{1-v^2}v^2\left(1-\frac{v^2}{3}\right)h_1(x,y)\times \left[\frac{1}{a_1}\,\mathrm{tg}^{-1}\frac{1}{a_1}-\frac{1}{2}\ln\frac{1+a_1^2}{a_1^2}\right]. \quad (19)$$

As in the case of the $\mu$-integrals above, we want to avoid double counting, and subtract the respective nonrelativistic contribution already accounted for in Eq. (6). This nonrelativistic contribution has the form

$$\Delta\epsilon^{(c)}_{\Sigma 1}(NR) = 3\int_0^1 dx\int_0^x dy\times \int_0^1 \frac{dv}{1-v^2}\,v^2\left(1-\frac{v^2}{3}\right)\frac{h_1(x,y)}{a_1}. \quad (20)$$

We now see that due to the identity

$$\mathrm{tg}^{-1}\left(\frac{1}{a_1}\right) = \frac{\pi}{2} - \mathrm{tg}^{-1}a_1,$$

subtraction of the nonrelativistic contribution from the integral in Eq. (19) reduces to the substitution

$$\mathrm{tg}^{-1}\left(\frac{1}{a_1}\right) \to -\,\mathrm{tg}^{-1}a_1. \quad (21)$$

This is a universal rule for subtraction of nonrelativistic contributions in all $c$-integrals considered below (cf. [5]). Finally, the first $c$-integral is

$$\Delta\epsilon^{(c)}_{\Sigma 1} - \Delta\epsilon^{(c)}_{\Sigma 1}(NR) = \int_0^1 dx\int_0^x dy\times \int_0^1 \frac{dv}{1-v^2}v^2\left(1-\frac{v^2}{3}\right)h_1(x,y)\times \left[-\frac{3}{a_1}\,\mathrm{tg}^{-1}a_1 - \frac{3}{2}\ln\frac{1+a_1^2}{a_1^2}\right] = -2.6215. \quad (22)$$

Next, we turn to the second $c$-integral defined in Eq. (10) and Eq. (8), and start with the momentum integration (cf. [4])

$$\Delta\epsilon^{(c)}_{\Sigma 2} = \int_0^1 dx\int_0^x dy\int_0^1 \frac{dv}{1-v^2}v^2\left(1-\frac{v^2}{3}\right)h_2(x,y)\times \int_0^\infty dk^2\left[\frac{(k^2+a_1^2)-\sqrt{(k^2+a_1^2)^2+4k^2}}{(k^2+a_1^2)^2} + \frac{1}{8k^2}\left(\sqrt{(k^2+a_1^2)^2+4k^2}-(k^2+a_1^2)-\frac{2k^2}{k^2+a_1^2}\right)\right] = \int_0^1 dx\int_0^x dy\int_0^1 \frac{dv}{1-v^2}v^2\left(1-\frac{v^2}{3}\right)h_2(x,y)\times \left[-\frac{2}{a_1}\,\mathrm{tg}^{-1}\frac{1}{a_1}+\frac{3}{4}\ln\frac{1+a_1^2}{a_1^2}+\frac{1}{4}-\frac{a_1^2}{4}\ln\frac{1+a_1^2}{a_1^2}\right]. \quad (23)$$

Subtraction of the nonrecoil contribution is needed to avoid double counting, and it is done with the help of universal rule Eq. (21). Then we obtain

$$\Delta\epsilon^{(c)}_{\Sigma 2} - \Delta\epsilon^{(c)}_{\Sigma 2}(NR) = \int_0^1 dx\int_0^x dy\times \int_0^1 \frac{dv}{1-v^2}v^2\left(1-\frac{v^2}{3}\right)h_2(x,y)\left[\frac{2}{a_1}\,\mathrm{tg}^{-1}a_1 + \frac{3}{4}\ln\frac{1+a_1^2}{a_1^2}+\frac{1}{4}-\frac{a_1^2}{4}\ln\frac{1+a_1^2}{a_1^2}\right] = 0.4370. \quad (24)$$

We now collect all contributions in Eqs. (6), (12), (18), (22), and (24) to obtain the total result for the contribution of the diagram with the self-energy insertion in Fig. 1:

$$\Delta\epsilon_\Sigma = \Delta\epsilon_\Sigma(NR) + (\Delta\epsilon^{(\mu)}_{\Sigma 1} - \Delta\epsilon^{(\mu)}_{\Sigma 1}(NR)) + (\Delta\epsilon^{(\mu)}_{\Sigma 2} - \Delta\epsilon^{(\mu)}_{\Sigma 2}(NR)) + \left(\Delta\epsilon^{(c)}_{\Sigma 1} - \Delta\epsilon^{(c)}_{\Sigma 1}(NR)\right) + \left(\Delta\epsilon^{(c)}_{\Sigma 2} - \Delta\epsilon^{(c)}_{\Sigma 2}(NR)\right) = \frac{0.4462}{\mu} + \frac{1}{6}\ln^3(2\mu) + \frac{1}{24}\ln^2(2\mu) + \left(\frac{13\pi^2}{12}-\frac{335}{36}\right)\ln(2\mu) - 0.1856. \quad (25)$$

### 2.2. Calculation of the spanning photon contribution

The contribution of the spanning photon diagrams in Fig. 1 is obtained from the contribution of the skeleton diagrams in Fig. 3 by insertion of a radiative photon with the polarization bubble, and is described by the expression (cf. [4])

$$\Delta\epsilon_\Xi = -\frac{i}{16\pi^2\mu^2}\int_0^1 dx \int_0^x dy(x-y)\int_0^1 \frac{dv}{1-v^2}v^2\left(1-\frac{v^2}{3}\right)\times \times \int \frac{d^4k}{k^4}\left(\frac{1}{k^2+\mu^{-1}k_0+i0}+\frac{1}{k^2-\mu^{-1}k_0+i0}\right)\left\{2(3k_0^2-2\mathbf{k}^2)\times \times\left[\frac{1-3y}{\Delta}+\frac{-k^2y^2(1-y)+2bk_0y^2(1-y)-2+x(2-x)(1-y)}{\Delta^2}\right]- - 6bk_0\left[\frac{3(1-y)}{\Delta}+\frac{k^2y(1-y)(2-y)-2bk_0y(1-y)^2+x(2-x)(1-y)}{\Delta^2}\right]\right\}, \quad (26)$$

where

$$\Delta(x,y) = y(1-y)(-k^2+2bk_0+a^2-i0), \quad a^2(x,y)=\frac{x^2+\lambda^2(1-x)}{y(1-y)}, \quad b(x,y)=\frac{1-x}{1-y}. \quad (27)$$

We simplify this expression using the identities

$$-k^2y^2(1-y)+2bk_0y^2(1-y)+x(2-x)(1-y) = = y\Delta+2x(1-y)-x^2-\lambda^2(1-x)y, \quad k^2y(1-y)(2-y)-2bk_0y(1-y)^2+ + x(2-x)(1-y) = -(2-y)\Delta + + 2bk_0y(1-y)+2x(1-y)+x^2+ + \lambda^2(1-x)(2-y), \quad (28)$$

and obtain

$$\Delta\epsilon_\Xi = -\frac{i}{16\pi^2\mu^2}\int_0^1 dx\int_0^x dy(x-y)\times \times\int_0^1\frac{dv}{1-v^2}v^2\left(1-\frac{v^2}{3}\right)\times \times\int\frac{d^4k}{k^4}\left(\frac{1}{k^2+\mu^{-1}k_0+i0}+\frac{1}{k^2-\mu^{-1}k_0+i0}\right)\times \times\left\{2(3k_0^2-2\mathbf{k}^2)\left[\frac{1-2y}{\Delta}+\frac{-2+2x(1-y)-x^2}{\Delta^2}+ + \frac{-\lambda^2(1-x)y}{\Delta^2}\right]-6bk_0\left[\frac{1-2y}{\Delta}+\frac{2x(1-y)+x^2}{\Delta^2}+ + \frac{\lambda^2(1-x)(2-y)}{\Delta^2}+\frac{2bk_0y(1-y)}{\Delta^2}\right]\right\}\equiv \equiv \Delta\epsilon_{\Xi1}+\Delta\epsilon_{\Xi2}, \quad (29)$$

where the contributions $\Delta\epsilon_{\Xi1}$ and $\Delta\epsilon_{\Xi2}$ correspond to the expressions in the first and second square brackets in the right-hand side of (29).

To calculate the integrals in Eq. (29), we use the same tricks as in the case of the mass operator contribution. We skip the calculation details and collect intermediate results in Table 1. Finally, we obtain the contribution of the diagram with the spanning photon insertion in Fig. 1 in the form

$$\Delta\epsilon_\Xi = \frac{0.4139}{\mu}+\frac{1}{6}\ln^3(2\mu)-\frac{5}{24}\ln^2(2\mu)+ + \left(\frac{\pi^2}{12}+\frac{13}{36}\right)\ln(2\mu)-0.6314. \quad (30)$$

### 2.3. Calculation of the vertex contribution

The contribution of the diagram with the vertex insertion in Fig. 1 is obtained from the contribution of the skeleton diagrams in Fig. 3 by insertion of the vertex function instead of one of the skeleton vertices. We have derived a convenient expression for the one-loop vertex function with a massive photon

$$\Lambda_\mu = \frac{\alpha}{2\pi}\int_0^1 dx\int_0^x\frac{dy}{\Delta}\gamma_\mu\times \times\left\{(k^2-2k_0)\Big[(x-y)(1-2y)+y(1-y)\Big]+ + 2\left(1-x-\frac{x^2}{2}\right)\frac{\Delta-\Delta_0}{\Delta_0}+ + (\not p-m)\,x(1-x)\frac{\Delta-\Delta_0}{\Delta_0}+ + 2k_0\Big[1-x+(x-y)^2\Big]-(\not p-\not k-m)(1-x)\right\} = = \sum_{i=1}^{i=5}\Lambda_\mu^{(i)}, \quad (31)$$

where

$$\Delta_0(x) = x^2+\lambda^2(1-x)$$

and the terms $\Lambda_\mu^{(i)}$ correspond to the five terms in the braces in Eq. (31).

This is essentially the same expression as the one in [4]. But unlike the respective expression in [4], where the photon mass merely served as a regularization parameter and was preserved only when necessary, we

**Table 1.** Spanning photon contributions

| | $\Xi 1$ | $\Xi 2$ |
|---|---|---|
| $\Delta\epsilon(NR)$ | $\dfrac{0.41386}{\mu} - 0.1186$ | 0.7213 |
| $\Delta\epsilon^{(\mu)} - \Delta\epsilon(NR)$ | $\frac{1}{6}\ln^3(2\mu) - \frac{5}{24}\ln^2(2\mu) + \left(\frac{\pi^2}{12} + \frac{13}{36}\right)\ln(2\mu) + \frac{1}{4}\zeta(3) - \frac{5\pi^2}{144} - \frac{9}{8} + 0.5259$ | 0 |
| $\Delta\epsilon^{(c)} - \Delta\epsilon(NR)$ | 0.1201 | −0.7130 |

here restored the full dependence on the finite photon mass $\lambda$ that effectively describes the polarization operator insertion. It can be shown that the gauge invariant anomalous magnetic moment does not generate radiative recoil corrections (see, e.g., [5, 7]). Therefore, the anomalous magnetic moment and some other terms that do not contribute to HFS are omitted in Eq. (31).

We insert the vertex in Eq. (31) into the skeleton expression for the contribution to HFS and obtain five integrals corresponding to the five terms in the right-hand side of (31). These integrals are calculated along the same lines as in the case of the mass operator discussed above in detail. We collect all intermediate results in Table 2. The total contribution of the diagram with the vertex insertion in Fig. 1 is given by

$$\Delta\epsilon_\Lambda = -\frac{1.1968}{\mu} - \frac{1}{6}\ln^3(2\mu) + \frac{11}{24}\ln^2(2\mu) + \left(-\frac{13\pi^2}{12} + \frac{80}{9}\right)\ln(2\mu) + 3.9489. \quad (32)$$

We now collect all the contributions in Eqs. (25), (30), and (32) generated by the diagrams with electron polarization insertions in Fig. 1 to obtain

$$\Delta\epsilon^{(e)} = \Delta\epsilon_\Sigma + 2\Delta\epsilon_\Lambda + \Delta\epsilon_\Xi = -\frac{1.5335}{\mu} + \frac{3}{4}\ln^2(2\mu) + \left(-\pi^2 + \frac{53}{6}\right)\ln(2\mu) + 7.0807. \quad (33)$$

The first term in the right-hand side is the well-known nonrecoil contribution to HFS [8], the second term is the leading logarithm squared contribution obtained in [9], and the single-logarithmic and constant terms are the subject of this work.

## 3. MUON POLARIZATION OPERATOR

Insertion of the muon polarization operator in the radiative photons in the diagrams in Fig. 2 lifts characteristic integration momenta to the scale of the muon mass. Hence, these diagrams do not generate nonrecoil contributions to HFS, all of which originate from the region of nonrelativistic muon momenta. Moreover, due to high characteristic momenta, these diagrams do not even generate recoil contributions logarithmic in the mass ratio that originate from the wide integration region between the electron and muon masses. As a result, the leading recoil contributions of the diagrams in Fig. 2 are pure numbers, and their calculation is significantly simpler than in the case of the electron polarization insertions in Fig. 1.

As in the previous section, insertion of the muon polarization operator in the diagrams in Fig. 2 is accounted for by the introduction of a photon mass, followed by an additional integration over the velocity with the weight in Eq. (1). For the muon polarization, the effective photon mass in the integrals is large,

$$\lambda^2 = \frac{4M^2}{1-v^2}$$

in dimensional units and it determines characteristic momenta in all the integrals. We can obtain the expressions for the energy shift due to muon polarization from the formulas for the respective electron polarization contributions above by rescaling the dimensionless integration momenta $k \to k/\mu$ (we recall that $\mu = m/2M$). In addition, we should adjust the expression for the photon mass; in terms of the rescaled integration momenta measured in units of $2M$, it is

$$\lambda^2 = \frac{1}{\mu^2(1-v^2)}.$$

After these substitutions, the expressions for the dimensionless contributions to HFS that are due to electron polarization become the expressions for the contributions due to muon polarization.

*a. Mass operator contribution.* To obtain an explicit expression for the diagrams with the mass operator insertions in Fig. 2, we rescale the integration momentum $k \to k/\mu$ in Eqs. (7) and (8), and redefine the photon mass squared as

**Table 2.** Vertex contributions

| | $\Delta\epsilon(NR)$ | $\Delta\epsilon^{(\mu)} - \Delta\epsilon(NR)$ | $\Delta\epsilon^{(c)} - \Delta\epsilon(NR)$ |
|---|---|---|---|
| $\Lambda 1$ | $-\frac{1.1356}{\mu} + 0.3385$ | $-\frac{1}{6}\ln^3(2\mu) + \frac{11}{24}\ln^2(2\mu) + \left(-\frac{5\pi^2}{12} + \frac{19}{8}\right)\ln(2\mu) + 3.2201$ | $-0.3315$ |
| $\Lambda 2$ | $-\frac{0.0507}{\mu} + 0.1007$ | $\left(\frac{2\pi^2}{3} - \frac{469}{72}\right)\ln\frac{M}{m} + 0.0371$ | $-0.0604$ |
| $\Lambda 3$ | $-\frac{0.0104}{\mu} + 0.0160$ | $-3\left(\frac{\pi^2}{3} - \frac{119}{36}\right)$ | $-0.0106$ |
| $\Lambda 4$ | $3.0460$ | $0$ | $-2.4323$ |
| $\Lambda 5$ | $-1.1758$ | $0$ | $1.1540$ |

$$\lambda^2 = \frac{1}{\mu^2(1-v^2)}.$$

The auxiliary functions used in Eqs. (7) and (8) are defined in Eq. (3). After rescaling, they simplify as

$$h_2(x,y) \to \frac{1-x}{y}, \quad a_1(x,y) \to \frac{1}{y\mu^2(1-v^2)}. \quad (34)$$

All the dependence on $\mu$ becomes explicit after these manipulations. It turns out that $\Delta\epsilon_{\Sigma 1}$ vanishes together with $\mu$. The total leading recoil contribution generated by the diagrams with the mass operator insertions in Fig. 2 coincides with $\Delta\epsilon_{\Sigma 2}$. Its calculation is straightforward, and we obtain

$$\Delta\epsilon_\Sigma = \int_0^1 dx \int_0^x dy \int_0^1 dv\, v^2 \left(1 - \frac{v^2}{3}\right) \times \int_0^\infty dk^2 \, \frac{1-x}{k^2 y(1-v^2)+1} \left[\frac{1}{k}\left(\sqrt{1+k^2}-k\right) - \frac{1}{2}\left(k\sqrt{1+k^2} - k^2 - \frac{1}{2}\right)\right] = 0.1329. \quad (35)$$

*b. Spanning photon contribution.* We obtain an expression for the spanning photon contribution with the muon polarization insertion in Fig. 2 by rescaling the integration momentum and the photon mass in Eq. (29). Under these transformations, the auxiliary function $\Delta(x,y)$ in Eq. (27) simplifies as

$$\Delta(x,y) \to \frac{y(1-y)}{\mu^2}\left[-k^2 + \frac{\mu^2\lambda^2(1-x)}{y(1-y)}\right]. \quad (36)$$

After rescaling, only the first and third terms in the first square bracket in the right-hand side of (29) produce contributions nonvanishing with $\mu$ contributions and we obtain

$$\Delta\epsilon_\Xi = \int_0^1 dx \int_0^x dy \int_0^1 dv\, v^2 \left(1 - \frac{v^2}{3}\right) \int_0^\infty dk^2 (x-y) \times \left[\frac{1-2y}{k^2 y(1-y)(1-v^2)+1-x} - \frac{(1-x)y}{[k^2 y(1-y)(1-v^2)+1-x]^2}\right] \times \left[\frac{1}{k}\left(\sqrt{1+k^2}-k\right) - \frac{1}{2}\left(k\sqrt{1+k^2} - k^2 - \frac{1}{2}\right)\right] = 0.3105. \quad (37)$$

*c. Vertex contribution.* Rescaling the integration momentum and the photon mass in the expressions corresponding to the five terms $\Lambda_\mu^{(i)}$, we obtain an explicit expression for the vertex diagram contribution in Fig. 2 to HFS. It is easy to see that after the rescaling, all the terms in the expression for the vertex function in Eq. (31) are suppressed by at least one power of $\mu$ in comparison with the first term. This means that only the first term generates the leading recoil correction in the case of a muon polarization insertion. Explicitly, the leading recoil correction generated by the vertex insertions in Fig. 2 has the form

$$\Delta\epsilon_\Lambda = -\int_0^1 dx \int_0^x dy \int_0^1 dv v^2 \left(1 - \frac{v^2}{3}\right) \times \int_0^\infty dk^2 \frac{(x-y)(1-2y) + y(1-y)}{k^2 y(1-y)(1-v^2)+1-x} \times \left[\frac{1}{k}\left(\sqrt{1+k^2}-k\right) - \frac{1}{2}\left(k\sqrt{1+k^2} - k^2 - \frac{1}{2}\right)\right] = -0.\,8738. \quad (38)$$

Collecting all the leading radiative recoil corrections in Eqs. (35), (37), and (38) corresponding to the diagrams with muon polarization insertions in Fig. 2, we obtain

$$\Delta\epsilon^{(\mu)} = \Delta\epsilon_\Sigma + 2\Delta\epsilon_\Lambda + \Delta\epsilon_\Xi = -1.3042. \qquad (39)$$

## 4. CONCLUSIONS

Restoring the overall dimensional factor in Eq. (33) and disregarding the nonrecoil and logarithm-squared terms known earlier, we obtain single-logarithmic and nonlogarithmic contributions to HFS generated by the diagrams with one-loop electron polarization insertions in Fig. 1:

$$\Delta E^{(e)} = \left[\left(\pi^2 - \frac{53}{6}\right)\ln\frac{M}{m} + 7.0807\right] \times \\ \times \frac{\alpha^2(Z\alpha)}{\pi^3}\frac{m}{M}E_F. \qquad (40)$$

The radiative recoil contribution generated by the diagrams with one-loop muon polarization insertions in Fig. 2 is nonlogarithmic. We obtain it by restoring the overall dimensional factor in Eq. (39):

$$\Delta E^{(\mu)} = -1.3042\,\frac{\alpha(Z^2\alpha)(Z\alpha)}{\pi^3}\frac{m}{M}E_F. \qquad (41)$$

The total contribution to HFS obtained above can be written as ($Z = 1$ in muonium)

$$\Delta E = \Delta E^{(e)} + \Delta E^{(\mu)} = \\ = \left[\left(\pi^2 - \frac{53}{6}\right)\ln\frac{M}{m} + 5.7765\right]\frac{\alpha^3}{\pi^3}\frac{m}{M}E_F. \qquad (42)$$

The theoretical accuracy of HFS in muonium is currently about 70 Hz. A realistic goal is to reduce this uncertainty to below 10 Hz (see a more detailed discussion in [1, 2]). The result in Eq. (42) together with other three-loop radiative recoil results in [10–12] makes this goal closer.

This work was supported by the NSF grant PHY-0757928. V. A. S. was also supported in part by the RFBR grants 06-02-16156 and 08-02-13516, and by the DFG grant GZ 436 RUS 113/769/0-3.

## REFERENCES

1. M. I. Eides, H. Grotch, and V. A. Shelyuto, *Theory of Light Hydrogenic Bound States*, Springer, Berlin, Heidelberg, New York (2007).

2. M. I. Eides, H. Grotch, and V. A. Shelyuto, Phys. Rep. **342**, 63 (2001).

3. M. I. Eides, H. Grotch, and V. A. Shelyuto, Can. J. Phys. **83**, 363 (2005).

4. S. G. Karshenboim, M. I. Eides, and V. A. Shelyuto, Yad. Fiz. **48**, 1039 (1988) [Sov. J. Nucl. Phys. **48**, 661 (1988)].

5. S. G. Karshenboim, V. A. Shelyuto, and M. I. Eides, Zh. Eksp. Teor. Fiz. **92**, 1188 (1987) [Sov. Phys.-JETP **65**, 664 (1987)].

6. V. B. Berestetskii, E. M. Lifshitz, and L. P. Pitaevskii, *Quantum Electrodynamics*, 2nd ed., Butterworth-Heinemann, Oxford (1999).

7. M. I. Eides, S. G. Karshenboim, and V. A. Shelyuto, Ann. Phys. (NY) **205**, 231 (1991).

8. M. I. Eides, S. G. Karshenboim, and V. A. Shelyuto, Phys. Lett. B **249**, 519 (1990); Pis'ma Zh. Eksp. Teor. Fiz. **52**, 937 (1990) [JETP Lett. **52**, 317 (1990)].

9. M. I. Eides, S. G. Karshenboim, and V. A. Shelyuto, Phys. Lett. B **216**, 405 (1989); Yad. Fiz. **49**, 493 (1989) [Sov. J. Nucl. Phys. **49**, 309 (1989)].

10. M. I. Eides, H. Grotch, and V. A. Shelyuto, Phys. Rev. D **65**, 013003 (2001).

11. M. I. Eides, H. Grotch, and V. A. Shelyuto, Phys. Rev. D **67**, 113003 (2003).

12. M. I. Eides, H. Grotch, and V. A. Shelyuto, Phys. Rev. D **70**, 073005 (2004).